

COB-2023-1544

THE USE OF MODERN INSTRUMENTS IN STRUCTURAL ANALYSIS : A REVIEW OF DIC AND FBG SENSORS

Vinicius Cruvinel Ferreira Vieira

Rodolpho Gardenal Fabbre

UNESP — São Paulo State University, Department of Mechanical Engineering, Centre for Simulation in Bioengineering, Biomechanics and Biomaterials (CS3B), School of Engineering, Campus of Bauru, São Paulo State, 17033-360, Brazil.

vinicius.cruvinel@unesp.br

rg.fabbre@unesp.br

Bruno Agostinho Hernandez

UNESP — São Paulo State University, Department of Mechanics, Centre for Simulation in Bioengineering, Biomechanics and Biomaterials (CS3B), School of Engineering, Campus of Guaratinguetá, São Paulo State, 12516-410, Brazil.

bruno.agostinho@unesp.br

Marcelo Sampaio Martins

UNESP — São Paulo State University, Department of Mechanics, Centre for Simulation in Bioengineering, Biomechanics and Biomaterials (CS3B), School of Engineering, Campus of Guaratinguetá, São Paulo State, 12516-410, Brazil.

sampaio.martins@unesp.br

Edson Capello Souza

UNESP — São Paulo State University, Department of Mechanical Engineering, Centre for Simulation in Bioengineering, Biomechanics and Biomaterials (CS3B), School of Engineering, Campus of Bauru, São Paulo State, 17033-360, Brazil.

edson.capello@unesp.br

Abstract. When there is a need for information regarding the state of stress and strain in a structure, electric strain gauges are commonly employed due to their affordability, accessibility, and versatility. However, this technique does have its drawbacks. It is susceptible to electrical interference, limited to specific temperature ranges, highly sensitive to mechanical impacts and high-frequency vibrations, and it is difficult to use it in remote locations. As a result, alternative strain measurement sensors have emerged, notably the Digital Image Correlation (DIC) and Fiber Bragg Grating (FBG) sensors. The primary objective of this study was to assess the current state art of DIC and FBG technologies. To achieve this, a comprehensive review of recent literature was conducted, considering the significant presence of both measurement methods on over 30,000 citations in articles published since 2022. DIC involves the use of a digital image correlation technique to analyze the surface of a structure while subjecting it to loading. By capturing and analyzing randomly spaced points through CCD cameras before, during, and after loading, the effects of deformations on the desired region can be accurately quantified. The advantages of DIC include its non-invasive and non-destructive nature, enabling analysis in both 2D and 3D, as well as the capability to measure objects of varying sizes. On the other hand, the FBG sensor serves as an alternative for stress, strain, pressure, temperature, and vibration analysis, among other parameters. It operates based on a refractive index modulation pattern within an optical fiber, forming Bragg gratings that act as wavelength filters. By analyzing the initial and reflected wavelength spectra in response to external stimuli, precise information regarding the monitored structure's properties can be obtained. Noteworthy advantages of the FBG sensor include its ability of multiplex, measuring multiple parameters simultaneously, its non-destructive nature, lightweight design, low cost maintenance, rapid and accurate response, high sensitivity, and immunity to electromagnetic interference. Considering the advantages offered by DIC and FBG sensors compared to strain gauges, it is intriguing to explore the use of these alternative sensing methods in deformation analysis, despite the high cost at the moment and lack of familiarity with the technology compared to electric strain gauges.

Keywords: structural analysis, Digital Image Correlation, DIC, Fiber Bragg Grating, FBG sensor

1. INTRODUCTION

When information about the state of stress and strain in a structure is needed, electric strain gauges are generally used due to their low cost, availability, and versatility. However, this technique has some disadvantages, such as sensitivity to electrical interference, operating within specific temperature ranges, high sensitivity to mechanical impacts and high-cycle vibrations, and difficulties in remote usage. As a result, other strain measurement sensors have emerged, such as Digital Image Correlation (DIC) and Fiber Bragg Grating (FBG) sensors. The aim of this study was to evaluate the state

of the art of DIC and FBG. This evaluation was carried out through a review of a wide range of recent papers on these methodologies, as both measurement modes have gained prominence with over 30,000 citations in articles published since 2022.

DIC is a measurement method that utilizes digital image correlation techniques to analyze the surface of a structure while it is subjected to loading. In the selected area, randomly spaced points allow software to analyze these points captured by CCD cameras before, during, and after loading, enabling the analysis pattern of deformations in the desired part and quantification of deformations at specific location. This method offers numerous advantages, including non-invasiveness, non-destructiveness, 2D and 3D deformation analysis capabilities, and the ability to measure objects of various sizes.

FBG sensors provide an alternative for analyzing stress, strain, pressure, temperature, vibrations, and other parameters. These optical sensors consist of a refractive index modulation pattern within an optical fiber, acting as wavelength filters called Bragg Gratings. By analyzing the wavelength spectra before and after reflections caused by perturbations, frequency changes can be detected and interpreted to provide accurate information about structure's properties. The FBG sensors offer advantages such as multiplexing, allowing the measurement of multiple parameters simultaneously, non-destructive testing, low weight, easy maintenance, rapid and precise responses, high sensitivity, and immunity to electromagnetic interference.

Therefore, incorporating other sensing methods like DIC and FBG in deformation analysis is beneficial due to their advantages over electric strain gauges. Electric strain gauges are widely used due to their affordability, availability, and versatility, but they have certain limitations. DIC provides non-invasive deformation analysis through image correlation, while FBG sensors utilize refractive index modulation to measure various parameters. Both methods have gained attention in deformation analysis and offer significant advantages over electric strain gauges. Advancements in these technologies have enabled more precise and comprehensive analysis of stress and strain in structures, providing valuable insights for industrial and structural applications in terms of design, monitoring, and maintenance.

2. TECHNOLOGIES

2.1 Fiber Bragg Grating Sensors

2.1.1 Historic Introduction

The introduction of fiber-optic communication has completely transformed various aspects of communication technology. Despite significant progress in this field, the integration of optical mirrors, partial reflectors, and wavelength filters presents a challenge due to increased complexity and cost. According to Sahota et al. (2020), this issue has been resolved through the utilization of fiber Bragg gratings. These gratings alone can fulfill essential functions such as reflection, dispersion, and filtering, making them highly adaptable for sensing applications. The photosensitivity process, which involves the optical absorption of ultraviolet (UV) light that alters the refractive index of the fiber core, is responsible for the formation of a fiber Bragg grating.

According to Chen et al. (2011), fiber optic sensors that utilize fiber Bragg gratings (FBGs) or arrays of FBGs have found extensive use in measuring various physical, chemical, biomedical, and electrical parameters. These sensors have gained particular significance in applications such as monitoring the structural health of civil infrastructures, aerospace systems, energy installations, and maritime environments. In these areas, the information about the measured quantities is typically encoded through the changes in the Bragg wavelength of the FBGs. This sensing approach offers numerous advantages, including its compact design, resistance to electromagnetic interference, ability to provide real-time monitoring with swift response, and exceptional sensitivity to external disturbances.

2.1.2 Theory Principle

Based on several articles, mainly from Chen et al. (2011), the working principle of a fiber Bragg grating (FBG) is based on creating a regular pattern of changes in the refractive index along the fiber's length. This pattern is achieved by exposing the fiber core to intense optical patterns. Think of it like creating a tiny, periodic structure within the fiber that acts as a specialized filter. When light passes through the fiber, only a specific narrow range of wavelengths is reflected back due to the interaction with these index changes. The point where this interaction is strongest is known as the Bragg wavelength, shown in Eq. (1). It's like a sweet spot where the reflection is most pronounced.

$$\lambda_B = 2\eta_{eff} \cdot \Lambda \quad (1)$$

Where λ_B is the Bragg wavelength of FBG, η_{eff} is the effective refractive index of the fiber core, and Λ represents the grating period. Both this Bragg wavelength and the operation of the FBG sensor can be observed in Figure 1.

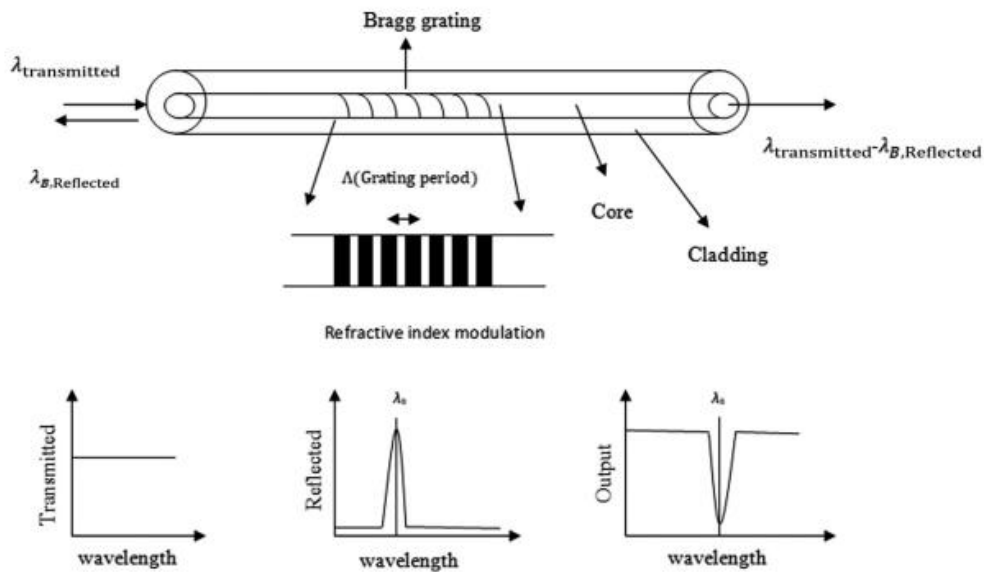


Figure 1. Structure of fiber Bragg grating along with the transmitted, reflected, and output spectra. Authors: Sahota (2020)

When the Bragg condition is fulfilled, the combined reflected light intensifies to create a peak in the backward direction, with its central wavelength determined by λ_B . The grating structure that adheres to the Bragg condition acts as a mirror, reflecting the specific wavelength λ_B and allowing the rest to pass through. According to Sahota et al. (2020), if the condition is not met, the reflections from the grating planes become out of phase and cancel each other out, resulting in no observable reflection. The reflectivity in FBG is calculated using Erdogan's coupled mode theory, which estimates the reflectivity $R_i(\lambda)$, shown in Eq. (2), at each grating within the fiber.

$$R_i(\lambda) = \frac{\sin^2(L_g \sqrt{k^2 - \sigma_i^2})}{\cos^2(L_g \sqrt{k^2 - \sigma_i^2}) - \frac{\sigma_i^2}{k^2}} \quad (2)$$

Where λ is the wavelength, k is the ac coupling coefficient between the two modes, L_g is the length of grating, product of k , and L_g gives strength of grating and for higher this value (for instance 8) the bandwidth of reflection spectra increases, and it is a unitless quantity. σ_i is the dc self-coupling coefficient, that gives the dependence of wavelength for every grating, and is given as

$$\sigma_i = \delta + \sigma - \frac{d\phi}{dz} \quad (3)$$

Where σ is the dc (period averaged) coupling coefficient, $\frac{d\phi}{dz}$ is the change in grating chirp, and δ is given as

$$\delta = 2\pi\eta_{eff} \left(\frac{1}{\lambda} - \frac{1}{\lambda_D} \right) \quad (4)$$

Where λ_D is the design wavelength for very weak gratings. When coupled mode theory is applied on reflectivity equation, Eq. (5) is obtained where $\delta\eta_{eff}$ gives magnitude of refractive index modulation

$$\sigma_i(\lambda) = \frac{\pi}{\lambda} \delta\eta_{eff} + 2\pi\eta_{eff} \left(\frac{1}{\lambda} - \frac{1}{\lambda_{B,i}} \right) \quad (5)$$

Sahota et al. (2020) further complements regarding the formation of these barriers, that to create gratings inside the fiber, there are different methods available, known as writing inside the fiber. Generally, there are two ways of writing: internal writing and external writing. Internal writing is not commonly used because it produces very small changes in the refractive index, which are not useful for practical applications. External writing, on the other hand, is the most commonly used method and can be done using different techniques like interferometers, phase masks, point-by-point, and line-by-line techniques.

2.1.3 Sensing Mechanism

The FBG sensor operates based on the concept of wavelength displacement. According to the theory of coupled mode, the Bragg wavelength is influenced by the physical characteristics of the fiber, including the period of the grating and the effective refractive index. A shift in the wavelength of the reflected spectrum, either towards the left or the right of the central wavelength, occurs only when there is a change in either the grating period or the effective refractive index of the FBG due to the parameter being measured, such as temperature, strain, humidity, pressure, and so on. By applying the Bragg condition, it is possible to identify changes in wavelength, which in turn indicate the level of external disturbance affecting the FBG.

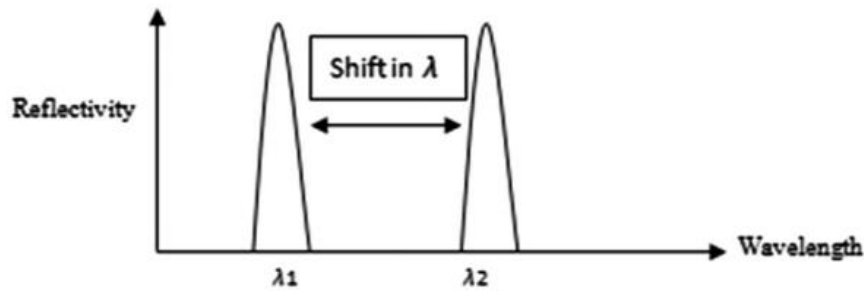


Figure 2. Wavelength shift due to external perturbation. Authors: Sahota et al. (2020)

In order to grasp the functioning of the sensing mechanism employed by FBG, let's explore an external factor referred to as "P," which corresponds to the measured quantity. This parameter could encompass variables such as temperature, strain, pressure, or refractive index. The Bragg wavelength of the FBG is contingent upon this external parameter, and its calculation involves differentiating Eq. (1) with respect to the "P" measurand, shown in Eq. (6)

$$\frac{d\lambda_B}{dP} = 2 \frac{d(\Delta\eta_{eff})}{dP} = 2\Delta \frac{d\eta_{eff}}{dP} + 2\eta_{eff} \frac{d\Delta}{dP} \quad (6)$$

As the Bragg wavelength relies on both the grating period and effective refractive index of the FBG, the measurand parameter will alter either the effective refractive index, the grating period, or both, contingent upon the specific type of measurand.

2.1.4 Multiplexing

One of the key advantages of FBG sensors is multiplexing. This feature enables the sensing of one or more parameters of interest along a single optical fiber, shown in Figure 3. This is possible because multiple sensors can be incorporated within the same fiber. With this ability to measure multiple equal or different parameters along the fiber, it provides a much more accurate and real-time monitoring of the analyzed situation.

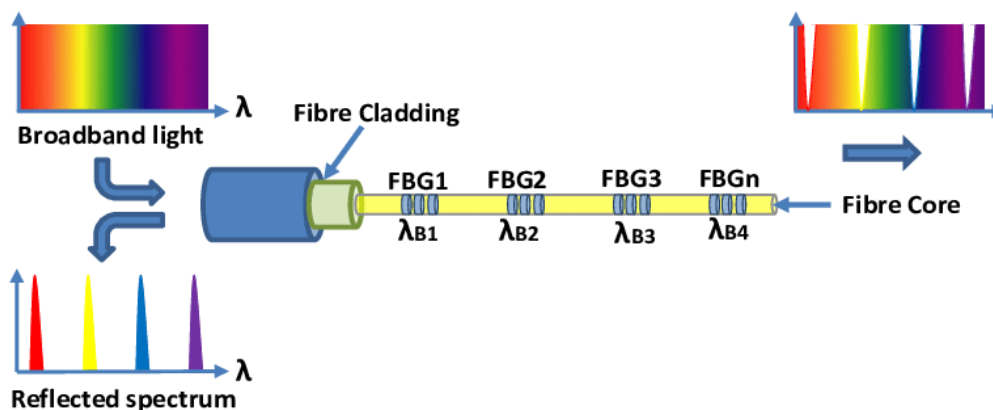


Figure 3. Operational principle of multiplexing in FBG sensors. Authors: Mohammed and Djurović (2018)

2.1.5 Applications

As seen in the previous sections, FBG sensors are highly versatile, precise, and reliable, making them suitable for various applications in both industry and research. In industrial settings, some areas where these sensors find application include:

Structural Monitoring: FBG sensors are used for structural health monitoring in various industries such as in constructions engineering, aerospace, and offshore structures. They can measure and monitor structural deformations, strains, and vibrations, providing valuable data for structural integrity assessment, shown in Figure 4.

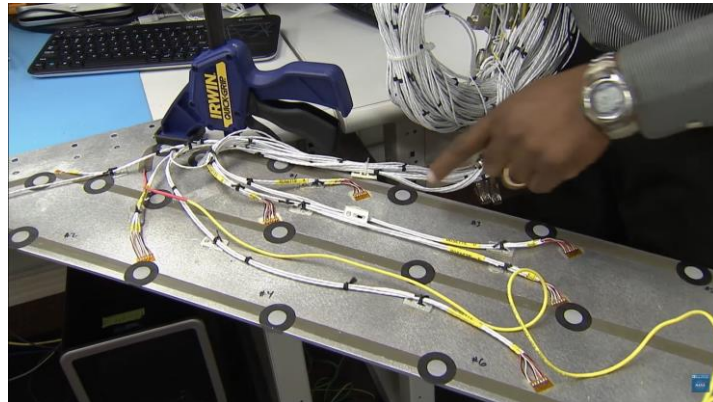


Figure 4. Airplane wing with markings of strain gauges and optical fiber with FBG sensors. Authors: [NASA Armstrong Flight Research Center]. (2015, February 22). *Fiber Optics Sensing System: A New Technology for Measurement* [Video]. Youtube. https://www.youtube.com/watch?v=_CdULw4-j_o&t=108s

Aerospace and Aviation: FBG sensors are employed in aircraft and spacecraft for monitoring various parameters like strain, temperature, and pressure. They help ensure the safety and reliability of critical components, such as wings, fuselage, and landing gears, shown in Figure 5.

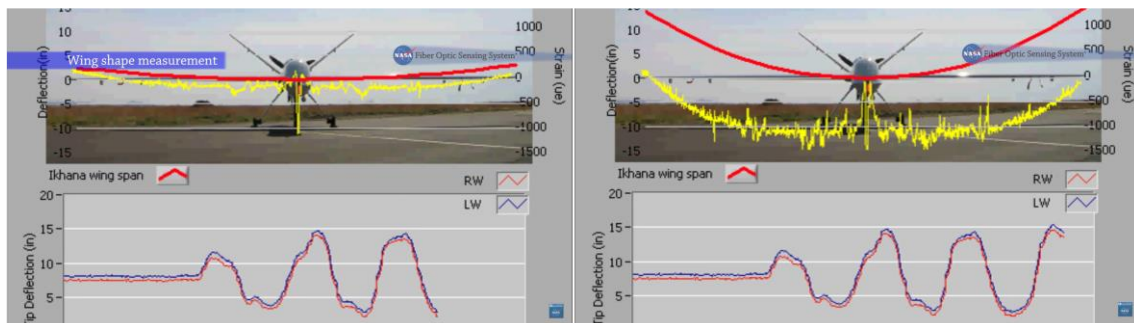


Figure 5. Relationship between the deflection of an airplane wing and its movement. Authors: [NASA Armstrong Flight Research Center]. (2015, February 22). *Fiber Optics Sensing System: A New Technology for Measurement* [Video]. Youtube. https://www.youtube.com/watch?v=_CdULw4-j_o&t=108s

Medical and Biomedical Applications: FBG sensors find applications in medical devices and biomedical research. They can be integrated into catheters, implants, and prosthetics to monitor parameters like strain, pressure, and temperature, providing valuable insights for diagnostics and treatment, shown in Figure 6.

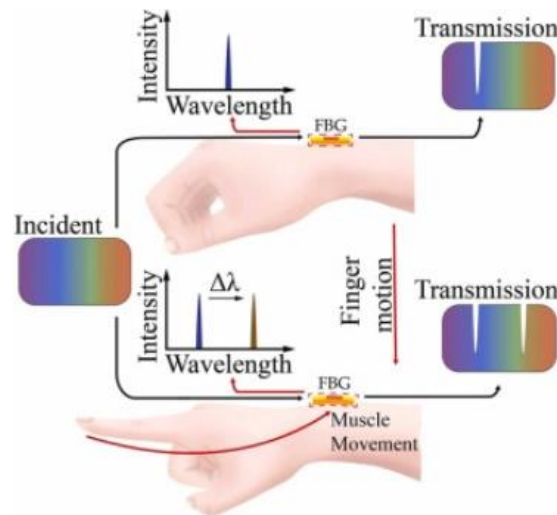


Figure 6. Operating principle of the FBG array sensor. Authors: Guo et al.(2022)

In addition to these main applications of FBG sensors, it is worth mentioning some other areas where their use is viable, such as: Oil and Gas Industry, Energy Sector, Automotive Industry and Smart Structures

2.2 Digital Image Correlation

2.2.1 Introduction

DIC is an optically-based technique used to measure the evolving full-field 2D or 3D coordinates on the surface of a test piece throughout a mechanical test. The measured coordinate fields can be used to calculate derived field quantities-of-interest (QOIs), such as displacements, strains, strain rates, velocities, and curvatures. Because DIC is a non-contact technique that is independent of the material being tested or the length-scale of interest, it can be used in a wide variety of applications to investigate and characterize the deformation of solids.

2.2.2 Historical introduction

Peters and Ranson, from the University of South Carolina, first proposed the idea of 2D Digital Image Correlation (DIC) in the field of experimental mechanics. In a article published in *Optical Engineering* in 1982, they tracked the rigid body movements of laser speckle patterns scattered on a small aluminum test specimen using a simple connectivity algorithm that combines the simplest form of cross-correlation (CC) function with the zeroth-order shape function. Throughout the 1980s, Peters (1983), Sutton (1983), Chu (1985), Sutton (1986), and their colleagues continued to enhance the original 2D DIC technique. In the 1990s, other advanced experimental techniques based on correlation were also proposed. For instance, to overcome the limitations of 2D DIC application and driven by practical requirements for measuring deformation on non-planar surfaces, stereo-DIC for 3D surfaces and deformation measurement, as well as DVC for truly full-field internal 3D deformation, were proposed. In the early 1990s, combining the principles of stereovision and 2D DIC, Luo et al. developed a two-camera stereovision system for surface deformation measurements. By the late 1990s, Bay (1999) aimed to recover 3D displacement and strain maps from 3D volumetric images of a bone specimen generated by high-resolution X-ray computed tomography (X-ray CT). Bay and colleagues successfully developed DVC for internal deformation measurement of objects with identifiable microstructures, which can be considered as a direct 3D extension of the subset-based 2D DIC method.

In the early 2000s, there was an increase in the usage of this technique, possibly due to the increasing computational capabilities of modern computers at decreasing costs, readily available image devices with improved performance, and the gradually accepted prominent advantages over interferometric optical techniques, along with the widespread acceptance of commercial DIC systems ready for use. Currently, DIC holds great relevance in the academic world, with over 400,000 citations in published documents over the past 5 years.

2.2.3 Principles of DIC

It is explained in Palanca (2016) that DIC uses digital images to track the displacement of portions of the speckled surface (Figure 7). In the case of 2D-DIC, images of specimen surface in the undeformed (or reference) and deformed states are acquired by one high-spatial-resolution digital image acquisition device (such as a regular digital camera, a high-speed camera, an optical microscope). The digital images (typically in grey scale) are divided into sub-images

(facets). In order to obtain an approximation of grey scale between pixels instead of discrete and independent values, the grey-scale distributions are interpolated, usually with a bicubic spline. Images of the deformed states are compared to the reference one in order to match facets and track the displacement.

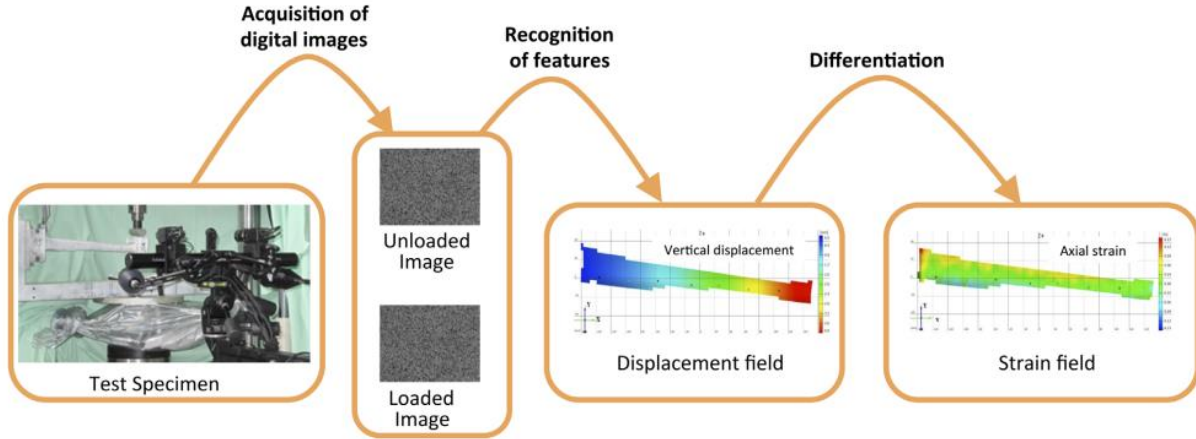


Figure 7. Workflow of DIC displacement and strain measurement: as an example, a 3D-DIC arrangement was used to investigate a human tibia. Authors: Palanca (2016)

The degree of matching between facets is evaluated by a normalized cross-correlation function such as Eq. (7):

$$\rho_{cc} = \frac{\sum_{i=1}^N \sum_{j=1}^M F(x_i, y_j) G(x'_i, y'_j)}{\sqrt{\sum_{i=1}^N \sum_{j=1}^M F^2(x_i, y_j) \sum_{i=1}^N \sum_{j=1}^M G^2(x'_i, y'_j)}}, \quad (7)$$

or a normalized sum-of-squared-differences such as Eq. (8):

$$\rho_{ssd} = \sum_{i=1}^N \sum_{j=1}^M \left[\frac{F(x_i, y_j)}{\sqrt{\sum_{i=1}^N \sum_{j=1}^M F^2(x_i, y_j)}} - \frac{G(x'_i, y'_j)}{\sqrt{\sum_{i=1}^N \sum_{j=1}^M G^2(x'_i, y'_j)}} \right]^2, \quad (8)$$

In this equation (Eq. 9), $F(x, y)$ and $G(x', y')$ represent the gray-scale values of pixels in the reference and deformed images, respectively. By matching facets, we automatically calculate the displacement by tracking the position changes of points on digitized images. The coordinates (x, y) and (x', y') describe the deformation between the two image states.

$$\begin{aligned} x' &= x + u + \frac{\partial u}{\partial x} \Delta x + \frac{\partial u}{\partial y} \Delta y, \\ y' &= y + v + \frac{\partial v}{\partial x} \Delta x + \frac{\partial v}{\partial y} \Delta y, \end{aligned} \quad (9)$$

In this equation (Eq. 9), we have variables u and v that represent the displacements of the facet centers in the x and y directions. These displacements show how the centers have moved. We also have Δx and Δy , which are the distances from the facet centers to a specific point defined by coordinates (x, y) . These distances help us understand where the point is located within the facet. The gradient terms in Eq. (9) indicate that the initial facet, which is made up of $M \times N$ pixels, is adjusted to match the corresponding facet in the deformed state. This matching process takes into account how the facet has strained or deformed. To measure the strain, we use the strain tensor described in Eq. (10). This tensor is obtained by analyzing the changes in displacement gradients. Previous studies have explored this process, such as the work by Sutton et al. (2009).

$$\begin{aligned} e_{xx} &= \frac{\partial u}{\partial x} + \frac{1}{2} \left[\left(\frac{\partial u}{\partial x} \right)^2 + \left(\frac{\partial v}{\partial x} \right)^2 \right], \\ e_{yy} &= \frac{\partial v}{\partial y} + \frac{1}{2} \left[\left(\frac{\partial u}{\partial y} \right)^2 + \left(\frac{\partial v}{\partial y} \right)^2 \right], \end{aligned} \quad (10)$$

$$\gamma_{xy} = \frac{1}{2} \left(\frac{\partial u}{\partial y} + \frac{\partial v}{\partial x} \right) + \frac{1}{2} \left[\left(\frac{\partial u}{\partial x} \right) \left(\frac{\partial u}{\partial y} \right) + \left(\frac{\partial v}{\partial x} \right) \left(\frac{\partial v}{\partial y} \right) \right],$$

In order to find the six deformation parameters and match the facet, an approximate-solution method is adopted. The Newton-Raphson algorithm is commonly used in displacement field analysis due to its computational efficiency (Kelley 1999). Another algorithm called Levenberg-Marquardt is also used in such analysis. These algorithms help converge to a solution where the displacement field can be obtained. However, sometimes there might be discontinuities in the field due to local variations in the grey-scale values. To address this issue and achieve a smooth and continuous displacement field, a smoothing algorithm is necessary. Different smoothing algorithms, such as those proposed by Wahba (1975) and Woltring (1985), are available. The choice of the appropriate algorithm depends on the characteristics of the noise that needs to be reduced, as discussed by Baldoni et al. (2015). In the case of three-dimensional digital image correlation (3D-DIC), it can be seen as an extension of 2D-DIC. The principles of operation are similar, but it incorporates a third dimension. This extension is achieved by utilizing stereoscopic vision with two or more cameras (Luo et al. 1992). By capturing images from different angles, 3D-DIC allows for the analysis of displacement and strain in all three dimensions. An example of a camera setup for image capture and data acquisition is presented in (Hernandez, 2019) by Figure 8.



Figure 8. Camera setup for image capture in an experiment. Authors: Hernandez (2019)

2.2.4 Application

The versatility of the digital image correlation (DIC) technique is evident in its wide range of applications across various industries and research fields. For instance, in the aerospace industry, DIC has been successfully employed to analyze and monitor the deformations of critical components, such as helicopter parts Luan (2022). In the field of biomechanics, DIC has revolutionized the study of *in vivo* tissues, enabling researchers to capture and quantify the intricate deformations occurring during physiological movements Palanca (2016). In the medical field, DIC has been instrumental in understanding the behavior of body parts under specific impact conditions. For example, researchers have used DIC to investigate the response of the cervical spine to mechanical shocks, shedding light on injury mechanisms and potential preventive measures Hernandez (2019) shown at Figure 9. This non-invasive technique provides invaluable insights into the complex deformation patterns within the human body. Furthermore, DIC has found practical applications in marine engineering, specifically in the analysis of propellers used underwater. By employing DIC, researchers can evaluate the performance and deformation characteristics of boat propellers, enabling optimization and improved efficiency Su (2022). The non-contact nature of DIC makes it particularly suitable for such underwater measurements as shown at Figure 10. In summary, the DIC technique has emerged as a versatile and powerful tool for capturing and analyzing deformations in a wide range of structures and materials. Its non-contact nature, high accuracy, and ability to provide full-field measurements make it a valuable asset in various fields, surpassing the limitations of traditional electrical strain gauges. As technology advances, DIC continues to evolve, opening up new possibilities for deformation analysis and contributing to advancements in research and industrial applications.

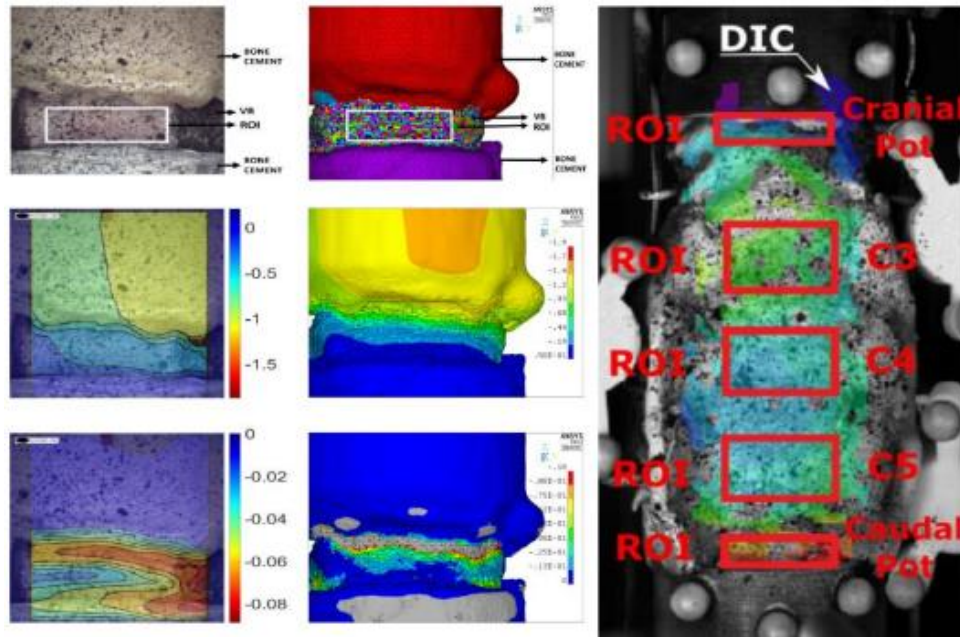


Figure 9. DIC analysis of the reaction of the cervical spine to mechanical shocks. Authors: Hernandez (2019)

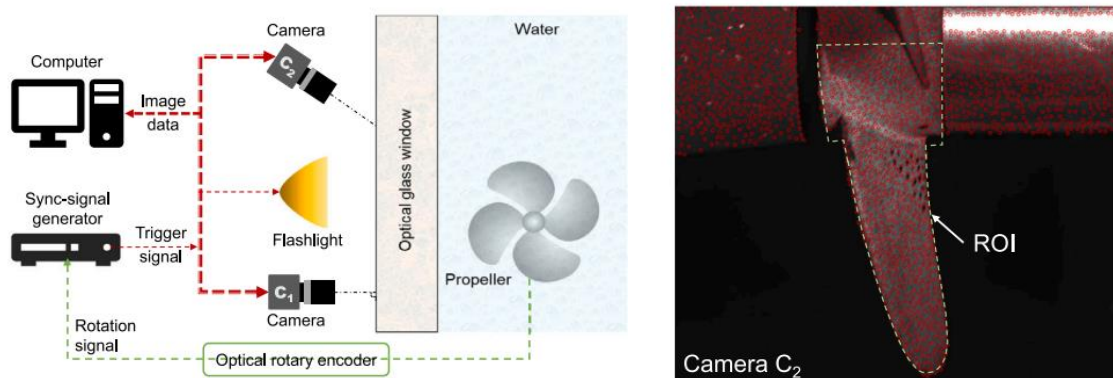


Figure 10. Schematic diagram of the rotation signal-controlled stroboscopic stereo-DIC system and samples of POIs extracted in the first image of camera used on the experiment. Authors: Su (2022)

3. CONCLUSION

In conclusion, Digital Image Correlation (DIC) and Fiber Bragg Grating (FBG) sensors offer significant advantages over electric strain gauges for deformation analysis. DIC analyzes surface deformations in 2D and 3D, while FBG sensors measure stress, strain, pressure, temperature, and vibrations with high sensitivity and immunity to interference. Both sensors provide multiplexing capabilities, non-destructive testing, lightweight design, easy maintenance, and rapid response. The growing recognition and adoption of DIC and FBG sensors highlight their importance in precise stress and strain assessment. Incorporating these sensors benefits industrial and structural applications by optimizing performance and ensuring system integrity.

4. ACKNOWLEDGEMENTS

We thank Prof. Edson Capello for giving us the opportunity to be part of CS3B - Center for Simulation in Bioengineering, Biomechanics, and Biomaterials, and professors Bruno Agostinho Hernandez and Marcelo Martins Sampaio for guiding us during this research. The authors gratefully acknowledge the support of the Brazilian Government and CAPES for a PIBIC student scholarship. Finally, we also extend our thanks to the Departments of Mechanical Engineering at School of Engineering of Bauru (FEB) and School of Engineering of Guaratinguetá (FEG), both from São Paulo State University "Júlio de Mesquita Filho" (UNESP).

5. REFERENCES

- Baldoni, J., Lionello G., Zama F., Cristofolini L. 2015. Comparison of different strategies to reduce noise in strain measurements with digital image correlation. *Meas Sci Technol* (under revision).
- Bay, Brian K., et al. "Measurement of strain distributions within vertebral body sections by texture correlation." *Spine* 24.1 (1999): 10-17.
- Bruck HA, McNeill SR, Sutton MA, Peters WH. 1989. Digital image correlation using Newton-Raphson method of partial differential correction. *Exp Mech*. Sept; 261-267
- Chen, J., Liu, B., & Zhang, H. (2011). Review of fiber Bragg grating sensor technology. *Frontiers of Optoelectronics in China*, 4, 204-212.
- Chu, T. C., W. F. Ranson, and Michael A. Sutton. "Applications of digital-image-correlation techniques to experimental mechanics." *Experimental mechanics* 25 (1985): 232-244.
- Guo, Y., Zhu, J., Xiong, L., & Guan, J. (2022). Finger motion detection based on optical fiber Bragg grating with polyimide substrate. *Sensors and Actuators A: Physical*, 338, 113482.
- Hernandez, Bruno Agostinho. A study of impact loading of the spine. 2019. PhD thesis, Mechanical Engineering Department - University of Bath, Bath, England, 2019
- Hill, K. O., Fujii, Y., Johnson, D. C., & Kawasaki, B. S. (1978). Photosensitivity in optical fiber waveguides: Application to reflection filter fabrication. *Applied physics letters*, 32(10), 647-649.
- Kelley CT. 1999. Iterative methods for optimization. Raleigh, NC: Society for Industrial and Applied Mathematics.
- Luan, L., Crosbie, L., MICHEL, S., & HACK, E. A Digital Image Correlation (DIC) prototype system for crack propagation monitoring in aircraft assemblies. *Open Research Europe*, v. 2, p. 82, 2022.
- Luo PF, Chao YJ, Sutton MA, Peters WH. 1992. Accurate measurement of three-dimensional deformations in deformable and rigid bodies using computer vision. *Exp Mech* June: 123-132
- Mohammed, A., & Djurović, S. (2018). A study of distributed embedded thermal monitoring in electric coils based on FBG sensor multiplexing. *Microprocessors and Microsystems*, 62, 102-109.
- Palanca, Marco, Gianluca Tozzi, and Luca Cristofolini. "The use of digital image correlation in the biomechanical area: a review." *International biomechanics* 3.1 (2016): 1-21.
- Peters WH, Ranson WF. 1982. Digital imaging techniques in experimental stress analysis. *Opt Eng*. 21:427-431.
- Peters, W. H., et al. "Application of digital correlation methods to rigid body mechanics." *Optical Engineering* 22.6 (1983): 738-742.
- Presti, D. L., Massaroni, C., Leitão, C. S. J., Domingues, M. D. F., Sypabekova, M., Barrera, D., ... & Schena, E. (2020). Fiber bragg gratings for medical applications and future challenges: A review. *Ieee Access*, 8, 156863-156888.
- Sahota, J. K., Gupta, N., & Dhawan, D. (2020). Fiber Bragg grating sensors for monitoring of physical parameters: A comprehensive review. *Optical Engineering*, 59(6), 060901-060901.
- Shen, W., Yan, R., Xu, L., Tang, G., & Chen, X. (2015). Application study on FBG sensor applied to hull structural health monitoring. *Optik*, 126(17), 1499-1504.
- Sutton MA, Orteu JJ, Schreier HW. 2009. Image correlation for shape, motion and deformation measurements. New York: Springer Science.
- Sutton, M. A., et al. "Determination of displacements using an improved digital correlation method." *Image and vision computing* 1.3 (1983): 133-139.
- Sutton, Michael A., et al. "Application of an optimized digital correlation method to planar deformation analysis." *Image and Vision Computing* 4.3 (1986): 143-150.
- SU, Zhilong, JIYU PAN, Shuiqiang Zhang, SHEN WU, Qifeng Yu, Zhang Dongsheng. Characterizing dynamic deformation of marine propeller blades with stroboscopic stereo digital image correlation. *Mechanical Systems and Signal Processing*, v. 162, p. 108072, 2022.
- Wang CCB, Deng J-M, Ateshian GA, Hung CT. 2002. An automated approach for direct measurement of two-dimensional strain distributions within articular cartilage under unconfined compression. *J Biomech Eng*. 124:557.
- Wahba G. 1975. Smoothing noisy data with spline functions. *Numer Math*. 24:383-393.
- Woltring HJ. 1985. On optimal smoothing and derivative estimation from noisy displacement data in biomechanics. *Hum Movement Sci*. 4:229-245.

6. RESPONSIBILITY NOTICE

The authors are the only responsible for the printed material included in this paper.